

# Skyrmion versus vortex flux lattices in $p$ -wave superconductors

Qi Li<sup>1</sup>, John Toner<sup>1</sup>, and D. Belitz<sup>1,2</sup>

<sup>1</sup>*Department of Physics and Institute of Theoretical Science, University of Oregon, Eugene, OR 97403*

<sup>2</sup>*Materials Science Institute, University of Oregon, Eugene, OR 97403*

(Dated: February 9, 2022)

$p$ -wave superconductors allow for topological defects known as skyrmions, in addition to the usual vortices that are possible in both  $s$ -wave and  $p$ -wave materials. In strongly type-II superconductors in a magnetic field, a skyrmion flux lattice yields a lower free energy than the Abrikosov flux lattice of vortices, and should thus be realized in  $p$ -wave superconductors. We analytically calculate the energy per skyrmion, which agrees very well with numerical results. From this, we obtain the magnetic induction  $B$  as a function of the external magnetic field  $H$ , and the elastic constants of the skyrmion lattice, near the lower critical field  $H_{c1}$ . Together with the Lindemann criterion, these results suffice to predict the melting curve of the skyrmion lattice. We find a striking difference in the melting curves of vortex lattices and skyrmion lattices: while the former is separated at all temperatures from the Meissner phase by a vortex liquid phase, the skyrmion lattice phase shares a direct boundary with the Meissner phase. That is, skyrmions lattices *never* melt near  $H_{c1}$ , while vortex lattices *always* melt sufficiently close to  $H_{c1}$ . This allows for a very simple test for the existence of a skyrmion lattice. Possible  $\mu$ SR experiments to detect skyrmion lattices are also discussed.

PACS numbers: 74.50.+r, 74.70.Pq, 74.25.Fy

## I. INTRODUCTION

One of the most fascinating phenomena exhibited by conventional,  $s$ -wave, type-II superconductors is the appearance of an Abrikosov flux lattice of vortices in the presence of an external magnetic field  $\mathbf{H}$  in a range  $H_{c1} < |\mathbf{H}| < H_{c2}$  between a lower critical field  $H_{c1}$  and an upper critical field  $H_{c2}$ .<sup>1</sup> It has been known for quite some time both theoretically<sup>2,3,4,5</sup> and experimentally<sup>6,7</sup> that these flux lattices can melt. The melting curve separates an Abrikosov vortex lattice phase from a vortex liquid phase, and the vortex lattice is found to melt in the vicinity of both  $H_{c1}$  and  $H_{c2}$ , as shown in Fig. 1. The melting occurs because the elastic constants of the flux lattice (i.e., the shear, bulk, and tilt moduli) vanish exponentially near these field values. As a result, in clean superconductors, root-mean-square positional thermal fluctuations  $\sqrt{\langle |\mathbf{u}(\mathbf{x})|^2 \rangle}$  grow exponentially as these fields are approached. According to the Lindemann criterion, when these fluctuations become comparable to the lattice constant  $a$ , the translational order of the flux lattice is destroyed; i.e., the lattice melts.

Vortices are topological defects in the texture of the superconducting order parameter, and in  $s$ -wave superconductors, where the order parameter is a complex scalar, only one type of defect is possible. In  $p$ -wave superconductors, the more complicated structure of the order parameter allows for an additional type of topological defect known as a skyrmion. In contrast to vortices, skyrmions do not involve a singularity at the core of the defect; rather, the order parameter field is smooth everywhere, as illustrated in Fig. 2. Skyrmions were first introduced in a nuclear physics context by Skyrme,<sup>8</sup> and slight variations of this concept<sup>9</sup> were later shown or proposed to be important in superfluid <sup>3</sup>He,<sup>10,11</sup> in the Blue Phases of

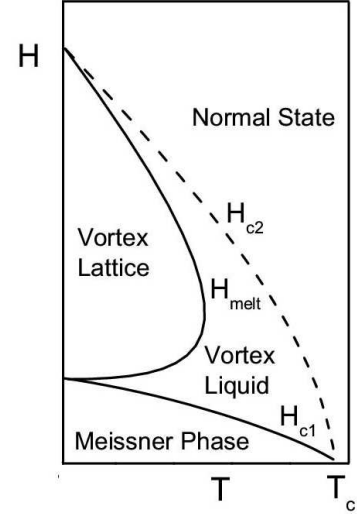


FIG. 1: External field ( $H$ ) vs. temperature ( $T$ ) phase diagram for vortex flux lattices. Shown are the Meissner phase, the vortex lattice phase, the vortex liquid, and the normal state. Notice that the vortex lattice is never stable sufficiently close to  $H_{c1}$ .

liquid crystals,<sup>12</sup> in Quantum Hall systems,<sup>13,14</sup> in itinerant ferromagnets,<sup>15</sup> and in  $p$ -wave superconductors.<sup>16</sup> In the latter case, skyrmions carry a quantized magnetic flux, as do vortices, although the lowest energy skyrmion contains two flux quanta, while the lowest energy vortex contains just one. For strongly type-II superconductors, skyrmions have a lower free energy than vortices, and a vortex lattice should thus be the state that occurs naturally.<sup>16</sup>

Recent evidence of  $p$ -wave superconductivity in  $\text{Sr}_2\text{RuO}_4$ <sup>17,18,19</sup> provides a motivation for further ex-

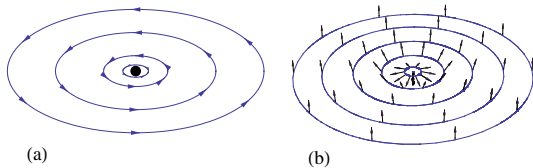


FIG. 2: Order parameter configurations showing a vortex (a), and a skyrmion (b). The local order parameters are represented by arrows on loci of equal distance from the center of the defect. If the order parameter space is two-dimensional, only vortices are possible, and there is a singularity at the center of each vortex, (a). If the order-parameter space is three-dimensional, a skyrmion can form instead, where the spin direction changes smoothly from “down” at the center to “up” at infinity, (b).

ploring the properties of skyrmion flux lattices in such systems.<sup>20</sup> It was shown numerically by Knigavko et al.<sup>16</sup> that the interaction between skyrmions falls off only as  $1/R$  with distance  $R$ , as opposed to the exponentially decaying interaction between vortices. As result, skyrmion lattices have a very different dependence of the magnetic induction on the external magnetic field near  $H_{c1}$  than do vortex lattices. In this paper we confirm and expand on these results. We show analytically that the skyrmion-skyrmion interaction, in addition to a leading  $1/R$ -dependence, has a correction proportional to  $\ln R/R^2$  that explains a small discrepancy between the numerical results in Ref. 16 and a strict  $1/R$  fit, and we calculate the interaction energy up to  $O(1/R^2)$ . We further show that the melting curve of a skyrmion lattice is qualitatively different from that of a vortex lattice. Namely, skyrmion lattices melt *nowhere* in the vicinity of  $H_{c1}$ , so there is a direct transition from the Meissner phase to the skyrmion lattice, see Fig. 8 below. Finally, we predict and discuss the magnetic induction distribution  $n(B)$  of a skyrmion lattice state as observed in a muon spin resonance ( $\mu$ SR) experiment. For a vortex lattice, the exponential decay of the magnetic induction  $B$  at large distances from a vortex core implies  $n(B) \propto \ln B/B$ . For a skyrmion lattice, we find that  $B$  decays only algebraically, which leads to  $n(B) \propto B^{-3/2}$ . Some of these results have been reported before in Ref. 21.

The paper is organized as follows. In Sec. II we review the formulation in Ref. 16 of the skyrmion problem. In particular, we start from the Ginzburg-Landau (GL) model for  $p$ -wave superconductors and consider the free energy in a London approximation. We parameterize the skyrmion solution of the saddle-point equations, and express the energy in terms of the solution of the saddle-point equations. In Sec. III we analytically solve these saddle-point equations perturbatively for large skyrmion radius  $R$ , and we calculate the energy of a single skyrmion as a power series in  $1/R$  to order  $1/R^2$ . In Sec. IV we

determine the elastic properties of the skyrmion lattice, and we predict the magnetic induction distribution  $n(B)$  as observed in a  $\mu$ SR experiment.

## II. FORMULATION OF THE SKYRMION PROBLEM

In this section we review the formulation of the skyrmion problem presented in Ref. 16, who derived an effective action that allows for skyrmions as saddle-point solutions. The resulting ordinary differential equations (ODEs) describing skyrmions<sup>16</sup> are the starting point for our analytic treatment.

### A. The action in the London approximation

We start from a Landau-Ginzburg-Wilson (LGW) functional appropriate for describing spin-triplet superconducting order,

$$S = \int d\mathbf{x} \mathcal{L}(\boldsymbol{\psi}(\mathbf{x}), \mathbf{A}(\mathbf{x})), \quad (2.1a)$$

with an action density

$$\begin{aligned} \mathcal{L}(\boldsymbol{\psi}, \mathbf{A}) = & t|\boldsymbol{\psi}|^2 + u|\boldsymbol{\psi}|^4 + v|\boldsymbol{\psi} \times \boldsymbol{\psi}^*|^2 + \frac{1}{2m}|\mathbf{D}\boldsymbol{\psi}|^2 \\ & + \frac{1}{8\pi}(\nabla \times \mathbf{A})^2. \end{aligned} \quad (2.1b)$$

Here  $\boldsymbol{\psi}(\mathbf{x})$  is a 3-component complex order parameter field,<sup>22</sup>  $\mathbf{A}(\mathbf{x})$  is the electromagnetic vector potential, and  $\mathbf{D} = \nabla - iq\mathbf{A}$  denotes the gauge invariant gradient operator.  $m$  and  $q$  are the mass and the charge, respectively, of a Cooper pair, and we use units such that  $\hbar = c = 1$ .  $t$ ,  $u$ , and  $v$  are the parameters of the LGW theory.

Let us look for saddle-point solutions to this action. In a large part of parameter space, namely, for  $v < 0$  and  $u > -v$ , the stable saddle-point solution is has the form  $\boldsymbol{\psi}(\mathbf{x}) \equiv \boldsymbol{\psi} = f_0(1, i, 0)/\sqrt{2}$ , where the amplitude  $f_0$  is determined by minimization of the free energy.<sup>23</sup> This is known as the  $\beta$ -phase, and it is considered the most likely case to be realized in any of the candidates for  $p$ -wave superconductivity.<sup>24</sup> Fluctuations about this saddle point are conveniently parameterized by writing the order parameter field as

$$\boldsymbol{\psi}(\mathbf{x}) = \frac{1}{\sqrt{2}} f(\mathbf{x}) (\hat{\mathbf{n}}(\mathbf{x}) + i\hat{\mathbf{m}}(\mathbf{x})), \quad (2.2)$$

where  $\hat{\mathbf{n}}(\mathbf{x})$  and  $\hat{\mathbf{m}}(\mathbf{x})$  are unit real orthogonal vectors in order-parameter space and  $f(\mathbf{x})$  is the modulus of order parameter. With this parameterization, the action density can be written

$$\begin{aligned} \mathcal{L} = & t f^2 + (u + v) f^4 \\ & + \frac{1}{2m} \left[ (\nabla f)^2 + f^2 \left[ \frac{1}{2} (\partial_i \hat{\mathbf{l}})^2 + (\hat{\mathbf{n}} \cdot \partial_i \hat{\mathbf{m}} - q A_i)^2 \right] \right] \\ & + \frac{1}{8\pi} (\nabla \times \mathbf{A})^2, \end{aligned} \quad (2.3)$$

where  $\hat{\mathbf{l}} = \hat{\mathbf{n}} \times \hat{\mathbf{m}}$ , summation over repeated indices is implied, and we have made use of the identities listed in Appendix A.

There are two length scales associated with the action density, Eq. (2.3). The coherence length  $\xi$  is determined by comparing the  $f^2$  term with the  $(\nabla f)^2$  term,

$$\xi = 1/\sqrt{2m|t|}. \quad (2.4a)$$

It is the length scale over which the amplitude of the order parameter will typically vary. The London penetration depth  $\lambda$  is determined by comparing the  $\mathbf{A}^2$  term with the  $(\nabla \times \mathbf{A})^2$  term,

$$\lambda = \sqrt{m/4\pi q^2 \langle f \rangle^2}. \quad (2.4b)$$

The ratio of these two length scales,  $\kappa \equiv \lambda/\xi$ , is the Ginzburg-Landau parameter. Now we write  $f(\mathbf{x}) = f_0 + \delta f(\mathbf{x})$ , with  $f_0 = \sqrt{-t/2(u+v)}$ . Deep inside the superconducting phase, where  $-t > 0$  is large, the amplitude fluctuations  $\delta f$  are massive, and to study low-energy excitations one can integrate out  $f$  in a tree approximation. This approximation becomes exact in the limit of large  $\kappa$  and is known in this context as the London approximation. We introduce dimensionless quantities by measuring distances in units of  $\lambda$  and the action in units of  $\Phi_0^2/32\pi^3\lambda$ , and we introduce a dimensionless vector potential  $\mathbf{a} = 2\pi\lambda\mathbf{A}/\Phi_0$ , with  $\Phi_0 = 2\pi/q$  the magnetic flux quantum. Ignoring constant contributions to the action we can then write the action density in London approximation as follows,<sup>16</sup>

$$\mathcal{L}_L = \frac{1}{2}(\partial_i \hat{\mathbf{l}})^2 + (\hat{\mathbf{n}} \partial_i \hat{\mathbf{m}} - a_i)^2 + \mathbf{b}^2, \quad (2.5)$$

with  $\mathbf{b} = \nabla \times \mathbf{a}$ . The above derivation makes it clear that this effective action is a generalization of the  $O(3)$  nonlinear sigma model (represented by the first term on the right-hand side of Eq. (2.5)) that one obtains for a real 3-vector order parameter by integrating out the amplitude fluctuations in tree approximation.<sup>25</sup>

## B. Saddle-point solutions of the effective action

We now are looking for saddle-point solutions to the effective field theory, Eq. (2.5). Considering  $\hat{\mathbf{l}}$  and  $\hat{\mathbf{n}}$  independent variables, and minimizing with respect to  $\hat{\mathbf{l}}$  subject to the constraints  $\hat{\mathbf{l}}^2 = \hat{\mathbf{n}}^2 = 1$  and  $\hat{\mathbf{l}} \cdot \hat{\mathbf{n}} = 0$  yields

$$\nabla^2 \hat{\mathbf{l}} - \hat{\mathbf{l}}(\hat{\mathbf{l}} \cdot \nabla^2 \hat{\mathbf{l}}) + 2J_i(\hat{\mathbf{l}} \times \partial_i \hat{\mathbf{l}}) = 0, \quad (2.6a)$$

with

$$\mathbf{J} = \nabla \times \mathbf{b} \quad (2.6b)$$

the supercurrent. The variation with respect to  $\mathbf{a}$  is straightforward and yields a generalized London equation,

$$a_i + J_i = \hat{\mathbf{n}} \partial_i \hat{\mathbf{m}}. \quad (2.6c)$$

It is convenient to take the curl of Eq. (2.6c) and use Eq. (A3) to express the right-hand side of the resulting equation in terms of  $\hat{\mathbf{l}}$ . We then obtain the saddle-point equations as a set of coupled partial differential equations (PDEs) in terms of  $\mathbf{b}$  and  $\hat{\mathbf{l}}$  only:

$$b_i - \nabla^2 b_i = \frac{1}{2} \epsilon_{ijk} \hat{\mathbf{l}} \cdot (\partial_j \hat{\mathbf{l}} \times \partial_k \hat{\mathbf{l}}), \quad (2.7a)$$

$$\nabla^2 \hat{\mathbf{l}} - \hat{\mathbf{l}}(\hat{\mathbf{l}} \cdot \nabla^2 \hat{\mathbf{l}}) + 2\epsilon_{ijk} \partial_j b_k (\hat{\mathbf{l}} \times \partial_i \hat{\mathbf{l}}) = 0. \quad (2.7b)$$

Notice that the right-hand side of Eq. (2.7a) is valid in this form only at points where  $\hat{\mathbf{l}}(\mathbf{x})$  is differentiable, see Eq. (A3). Field configurations that obey these PDEs have an energy

$$E = \int d\mathbf{x} \left[ \frac{1}{2}(\partial_i \hat{\mathbf{l}})^2 + (\hat{\mathbf{n}} \cdot \partial_i \hat{\mathbf{m}} - a_i)^2 + \mathbf{b}^2 - 2\mathbf{h} \cdot \mathbf{b} \right]. \quad (2.8)$$

where we have added a uniform external magnetic field  $\mathbf{h}$  measured in units of  $\Phi_0/2\pi\lambda^2$ . Notice that the energy depends on  $\hat{\mathbf{n}}$  and  $\hat{\mathbf{m}}$ , whereas Eqs. (2.7) depend only on  $\hat{\mathbf{l}}$ , and that different choices of  $\hat{\mathbf{n}}$  and  $\hat{\mathbf{m}}$  can lead to the same  $\hat{\mathbf{l}}$ . Therefore, a field configuration satisfying Eqs. (2.7) is only necessary for making the energy stationary, but not sufficient.

### 1. Meissner solution

A very simple order parameter configuration consists of constant  $\hat{\mathbf{n}}(\mathbf{x})$  and  $\hat{\mathbf{m}}(\mathbf{x})$  everywhere, see Fig. 3. This

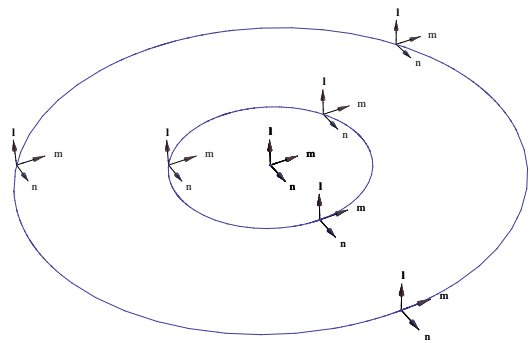


FIG. 3: Configurations of the vectors  $\hat{\mathbf{l}}$ ,  $\hat{\mathbf{m}}$ , and  $\hat{\mathbf{n}}$  in a Meissner phase. All three vectors point in the same direction everywhere.

leads to an  $\hat{\mathbf{l}}(\mathbf{x}) \equiv \hat{\mathbf{l}}$  that is constant everywhere. Equation (2.7b) is then trivially satisfied. The right-hand side of Eq. (2.7a) vanishes, and hence the PDE for  $\mathbf{b}$  reduces to the usual London equation with a solution  $\mathbf{b}(\mathbf{x}) \equiv 0$  in the bulk. This solution describes a Meissner phase with energy  $E_M = 0$ .

## 2. Vortex solution

Now consider a field configuration where  $\hat{\mathbf{n}}(\mathbf{x})$  and  $\hat{\mathbf{m}}(\mathbf{x})$  are confined to a plane (say, the  $x$ - $y$  plane), but rotate about an arbitrarily chosen point of origin:

$$\begin{aligned}\hat{\mathbf{n}}(\mathbf{x}) &= (\cos \phi, \sin \phi, 0), \\ \hat{\mathbf{m}}(\mathbf{x}) &= (-\sin \phi, \cos \phi, 0),\end{aligned}\quad (2.9)$$

where  $\phi$  denotes the azimuthal angle in the  $x$ - $y$  plane with respect to the  $x$ -axis. This field configuration, known as a vortex and shown in Fig. 4, corresponds to a constant  $\hat{\mathbf{l}}$  everywhere except at the origin, where there is a singularity. Therefore, the right-hand side of Eq. (2.7a) is not

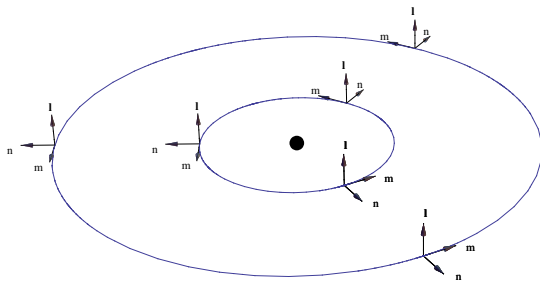


FIG. 4: Configurations of the vectors  $\hat{\mathbf{l}}$ ,  $\hat{\mathbf{m}}$ , and  $\hat{\mathbf{n}}$  for a vortex.  $\hat{\mathbf{l}}$  is constant, whereas  $\hat{\mathbf{m}}$  and  $\hat{\mathbf{n}}$  rotate about the vortex core. Notice that the vector shown in Fig. 2(a) is  $\hat{\mathbf{n}}$ .

applicable, and we return to Eq. (2.6c), which takes the form

$$a_i + \epsilon_{ijk} \partial_j a_k = \partial_i \phi. \quad (2.10)$$

For any closed path  $\mathcal{C}$  in the  $x$ - $y$  plane that surrounds the origin one has

$$\oint_{\mathcal{C}} d\ell \cdot \nabla \phi(\mathbf{x}) = 2\pi, \quad (2.11a)$$

or, by Stokes' theorem,

$$\int_{\mathcal{A}} d\mathbf{s} \cdot (\nabla \times \nabla \phi(\mathbf{x})) = 2\pi, \quad (2.11b)$$

where  $\mathcal{A}$  is the surface whose boundary is  $\mathcal{C}$ .<sup>26</sup> This quantization condition shows that, instead of Eq. (2.7a), we have

$$\mathbf{b}(\mathbf{x}) - \nabla^2 \mathbf{b}(\mathbf{x}) = 2\pi \hat{\mathbf{z}} \delta(x) \delta(y). \quad (2.12)$$

This is solved by a  $\mathbf{b}$  that is equal to the boundary condition value everywhere along the  $z$ -axis and that falls off exponentially away from the  $z$ -axis. This solution is known as a vortex, and the amount of magnetic flux contained in one vortex is one flux quantum  $\Phi_0$ .<sup>26</sup> It is the

precise analog of, and, indeed, essentially identical to, the familiar vortex in conventional  $s$ -wave superconductors.

The energy of a vortex given by Eq. (2.12), as calculated from Eq. (2.8), is logarithmically infinite. This is due to the point-like nature of the vortex core where the amplitude of the order parameter goes discontinuously to zero. In reality, the amplitude cannot vary on length scales shorter than the coherence length  $\xi$ , which provides an ultraviolet cutoff. The energy is then proportional to  $\ln \kappa$ .<sup>1</sup> In an external magnetic field this energy cost is offset by the magnetic energy gain due to letting some flux penetrate the sample. For  $\kappa$  larger than a critical value  $\kappa_c = 1/\sqrt{2}$ , and for external fields larger than the lower critical field  $H_{c1}$ , a hexagonal lattice of vortices has a lower energy than the Meissner phase. This state is known as an Abrikosov flux lattice,

and is precisely the same as that in conventional  $s$ -wave superconductors.<sup>1</sup>

## 3. Skyrmion solution

Due to the three-component nature of the order parameter, more complicated solutions of the saddle-point equations can be constructed for which the vector  $\hat{\mathbf{l}}$  is not fixed. Let  $\theta$  be the angle between  $\hat{\mathbf{l}}$  and the  $z$ -axis, and consider a cylindrically symmetric field configuration parameterized as

$$\begin{aligned}\hat{\mathbf{l}} &= \hat{\mathbf{e}}_z \cos \theta(r) + \hat{\mathbf{e}}_r \sin \theta(r), \\ \hat{\mathbf{n}} &= (\hat{\mathbf{e}}_z \sin \theta(r) - \hat{\mathbf{e}}_r \cos \theta(r)) \sin \varphi + \hat{\mathbf{e}}_\varphi \cos \varphi \\ \hat{\mathbf{m}} &= (\hat{\mathbf{e}}_z \sin \theta(r) - \hat{\mathbf{e}}_r \cos \theta(r)) \cos \varphi - \hat{\mathbf{e}}_\varphi \sin \varphi.\end{aligned}\quad (2.13)$$

For this to minimize the energy,  $\hat{\mathbf{l}}$  at large distances from the origin must be constant because of the first term in the energy, Eq. (2.8), and for a skyrmion centered in a cylinder of radius  $R$  we take  $\hat{\mathbf{l}}$  to point in the  $+z$ -direction for  $r = R$ ,  $\theta(r = R) = 0$ . The quantization condition analogous to Eq. (2.11b) for the vortex is<sup>27,28</sup>

$$\int dx dy \epsilon_{ij} \hat{\mathbf{l}} \cdot (\partial_i \hat{\mathbf{l}} \times \partial_j \hat{\mathbf{l}}) = 8\pi \quad (2.14)$$

To be consistent with this,  $\hat{\mathbf{l}}$  must point in the  $-z$ -direction at the origin,  $\theta(r = 0) = \pi$ .

Equation (2.13) parameterizes the order parameter in terms of a function  $\theta(r)$ . In addition, the energy depends on the vector potential which we take to be purely azimuthal, in accordance with our cylindrically symmetric *ansatz*,

$$\mathbf{a}(\mathbf{x}) = a(r) \hat{\mathbf{e}}_\varphi. \quad (2.15)$$

With this parameterization, we obtain from Eq. (2.8) the energy per unit length, along the cylinder axis, of a

cylindrically symmetric skyrmion in a region of radius  $R$ ,

$$\begin{aligned} E/E_0 &= \frac{1}{2} \int_0^R dr r \left[ (\theta'(r))^2 + \frac{1}{r^2} \sin^2 \theta(r) \right] \\ &+ \int_0^R dr r \left[ \frac{1}{r} (1 + \cos \theta(r)) + a(r) \right]^2 \\ &+ \int_0^R dr r \left[ \frac{a(r)}{r} + a'(r) \right]^2, \end{aligned} \quad (2.16)$$

where  $E_0 = (\Phi_0/4\pi\lambda)^2$ . This expression was first obtained in Ref. 16. The three terms correspond to the three terms in the London action, Eq. (2.5). They represent the energy of the nonlinear sigma model, the kinetic energy of the supercurrent, and the magnetic energy, respectively. Minimization of  $E$  with respect to  $\theta(r)$  and  $a(r)$  yields Euler-Lagrange equations

$$\theta''(r) + \frac{1}{r} \theta'(r) = \frac{-\sin \theta(r)}{r} \left[ \frac{2 + \cos \theta(r)}{r} + 2a(r) \right], \quad (2.17a)$$

$$a''(r) + \frac{1}{r} a'(r) - \frac{1}{r^2} a(r) = a(r) + \frac{1}{r} [1 + \cos \theta(r)]. \quad (2.17b)$$

This set of coupled, nonlinear ODEs must be solved subject to the boundary conditions  $\theta(r=0) = \pi$  and  $\theta(r=R) = 0$ , as explained above. The solution is known as a skyrmion, and each skyrmion contains two flux quanta.<sup>28</sup> Since Eqs. (2.7) are necessary for making the energy stationary, the solution of Eqs. (2.17), inserted in Eqs. (2.13, 2.15), is guaranteed to be a solution of Eqs. (2.7) as well.

The energy of a single skyrmion is finite even in London approximation, see Sec. III below. For large values of the Ginzburg-Landau parameter  $\kappa$  a skyrmion therefore has a lower energy than a vortex and the value of the lower critical field  $H_{c1}$ , at which the Meissner phase becomes unstable, is correspondingly lower for skyrmions than for vortices. This is the basis for the expectation that, in strongly type-II (i.e., large- $\kappa$ )  $p$ -wave superconductors, a skyrmion flux lattice will be realized rather than a vortex flux lattice.

### III. ANALYTIC SOLUTION OF THE SINGLE-SKYRMION PROBLEM

We now need to solve the coupled ODEs (2.17). Due to their nonlinear nature, this is a difficult task, and in Ref. 16 it was done numerically. It turns out, however, that one can construct a perturbative analytical solution in the limit of large skyrmion radius,  $R \gg \lambda$ , with  $\lambda/R$  as a small parameter. This provides information about the superconducting state near  $H_{c1}$ , where the system is always in that limit. We will construct the perturbative solution, and calculate the energy, to second order in the small parameter. Our general strategy is as follows. We

use Eq. (2.17b) to iteratively express  $a$  in terms of  $\theta$  and its derivatives. Substitution in Eq. (2.17a) then yields a closed ODE for  $\theta(r)$  that has to be solved.

#### A. Zeroth order solution

Let us first consider  $R = \infty$ . For  $r \rightarrow \infty$ , the left-hand side of Eq. (2.17b) falls off as  $1/r^2$ , and hence the vector potential, to zeroth order for large  $r$ , is given by

$$a_\infty(r) = -\frac{1}{r} [1 + \cos \theta(r)]. \quad (3.1)$$

Note that we use the *exact*  $\theta(r)$  in this expression, *not* the zeroth order approximation to it. Since we can only compute  $\theta(r)$  perturbatively, this expression for the zeroth order vector potential will itself have to be expanded perturbatively later. Substitution in Eq. (2.17a) yields

$$r^2 \theta''(r) + r \theta'(r) = \frac{1}{2} \sin(2\theta(r)). \quad (3.2)$$

The solution obeying the appropriate boundary condition is<sup>16</sup>

$$\theta_\infty(r) = f(r/\ell), \quad (3.3a)$$

with

$$f(x) = 2 \arctan(1/x). \quad (3.3b)$$

The length scale  $\ell$  is arbitrary at this point and will be determined later from the requirement  $\theta(r=R < \infty) = 0$ . For  $R \gg 1$  it will turn out that  $\ell \propto \sqrt{R}$ . The skyrmion solution is schematically shown in Fig. 5.

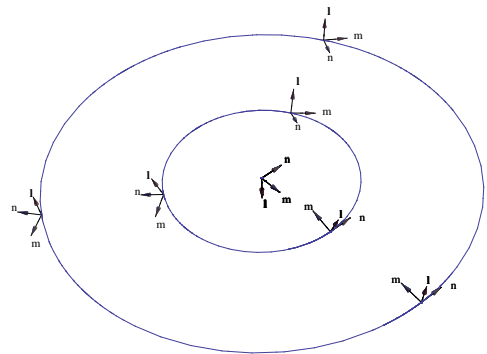


FIG. 5: Configurations of the vectors  $\hat{\ell}$ ,  $\hat{m}$ , and  $\hat{n}$  for a skyrmion. Notice that the vector shown in Fig. 2(b) is  $\hat{\ell}$ .

#### B. Perturbation theory for $R \gg 1$

We now determine the corrections to the zeroth order solution. Let us write  $\theta(r) = \theta_\infty(r) + \delta\theta(r)$  and

$a(r) = a_\infty(r) + \delta a(r)$  and require  $|\delta a(r)| \ll |a_\infty(r)|$  and  $|\delta\theta(r)| \ll 1$ .<sup>29</sup> An inspection of the ODEs (2.17) shows that for  $r \lesssim O(\ell)$ , the corrections can be expanded in a series in powers of  $1/\ell$ ,

$$\delta\theta(r) = \frac{1}{\ell^2} g(r/\ell) + \frac{1}{\ell^4} h(r/\ell) + O(1/\ell^6), \quad (3.4a)$$

$$\delta a(r) = \frac{1}{\ell^3} \alpha(r/\ell) + \frac{1}{\ell^5} \beta(r/\ell) + O(1/\ell^7). \quad (3.4b)$$

The functions  $\alpha$  and  $\beta$  can be determined by substituting Eq. (3.4b) in Eq. (2.17b) and equating coefficients of powers of  $1/\ell$ . The resulting equations for  $\alpha$  and  $\beta$  are linear *algebraic* equations, not ODE's, because terms involving derivatives of  $\alpha$  and  $\beta$  only enter at higher order in  $1/\ell$ , as one can verify by direct calculation. Hence, the solutions for  $\alpha$  and  $\beta$  can be read off at once, and are:

$$\alpha(x) = \frac{16x}{(1+x^2)^3}, \quad (3.5a)$$

$$\begin{aligned} \beta(x) = & 2 \frac{(3x^4 - 6x^2 - 1)}{x^2(1+x^2)^3} g(x) - 2 \frac{(3x^2 - 1)}{x(1+x^2)^2} g'(x) \\ & + \frac{2}{1+x^2} g''(x) + A(x), \end{aligned} \quad (3.5b)$$

where

$$\begin{aligned} A(x) &= \alpha''(x) + \frac{1}{x} \alpha'(x) - \frac{1}{x^2} \alpha(x) \\ &= \frac{384x(x^2 - 1)}{(1+x^2)^5}. \end{aligned} \quad (3.5c)$$

Similarly, by comparing coefficients in Eq. (2.17a) we find ODEs for the functions  $g$  and  $h$ ,

$$g''(x) + \frac{1}{x} g'(x) - \frac{1}{x^2} \cos(2f(x)) g(x) = -\frac{2}{x} \sin(f(x)) \alpha(x), \quad (3.6a)$$

$$h''(x) + \frac{1}{x} h'(x) - \frac{1}{x^2} \cos(2f(x)) h(x) = -\frac{2}{x} \sin(f(x)) \beta(x) - \frac{1}{x^2} \sin(2f(x)) g^2(x) - \frac{2}{x} \cos(f(x)) \alpha(x) g(x), \quad (3.6b)$$

with  $f(x)$  from Eq. (3.6b).

The ODE (3.6a) for  $g$  can be solved by standard methods, see Appendix B. The physical solution is the one that vanishes for  $x \rightarrow 0$ ; it is proportional to  $x$  for  $x \gg 1$ . We find

$$g(x) = -\frac{4}{3} \frac{x[x^2(4+x^2) + 2(1+x^2)\ln(1+x^2)]}{(1+x^2)^2}, \quad (3.7a)$$

the large- $x$  asymptotic behavior of which is

$$g(x \gg 1) = -\frac{4}{3} x - \frac{16}{3} \frac{\ln x}{x} - \frac{8}{3x} + O\left(\frac{\ln x}{x^2}\right). \quad (3.7b)$$

This determines both the function  $\beta(x)$ , Eq. (3.5b), and the inhomogeneity of the ODE (3.6b) for  $h(x)$ . The latter can again be solved in terms of tabulated functions, see Appendix B, but we will need only the two leading terms for  $x \rightarrow \infty$ . The physical solution is again the one that vanishes for  $x \rightarrow 0$ , and its large- $x$  asymptotic behavior is

$$h(x \gg 1) = -\frac{32}{9} x \ln x + \frac{536}{135} x + O(1/x). \quad (3.8)$$

Finally, we need to fix the length scale  $\ell$ . It is determined by the requirement  $\theta(r = R) = 0$ . We find

$$\ell^2 = \sqrt{\frac{c}{2}} R \left[ 1 + \frac{\sqrt{2c}}{R} \ln R + \frac{\delta}{R} + O\left(\frac{\ln R}{R^{3/2}}\right) \right], \quad (3.9a)$$

where

$$\delta = \sqrt{2c} \left[ \frac{1}{12} (7 - 6d/c^2) - \frac{1}{2} \ln(c/2) \right], \quad (3.9b)$$

and

$$c = 4/3, \quad (3.9c)$$

$$d = 536/135, \quad (3.9d)$$

are the absolute values of the coefficients of the terms proportional to  $x$  in the large- $x$  expansions of  $g(x)$  and  $h(x)$ , respectively. We see that, for  $R \gg 1$ ,  $\ell$  is indeed proportional to  $\sqrt{R}$ , as we had anticipated above. That is, the characteristic skyrmion length scale  $\ell$  is the geometric mean of the London penetration depth  $\lambda$  (recall that we measure all lengths in units of  $\lambda$ ) and the skyrmion size  $R$ . We now can also check our requirement  $\delta\theta \ll 1$ : from

Eq. (3.4a) we see that for  $r \ll \ell$ ,  $\delta\theta(r) \propto 1/R$ , while for  $r \gg \ell$ ,  $\delta\theta(r)$  is bounded by a term proportional to  $1/R^{1/2}$ . For  $R$  large compared to the penetration depth the condition is thus fulfilled for all  $r$ . Similarly,  $\delta a$  is found to be small compared to  $a_\infty$  for all  $r$ .

### C. Energy of a single skyrmion

By using our perturbative solution in Eq. (2.16), we are now in a position to calculate the energy of a single skyrmion to  $O(1/R^2)$ . It is convenient to first expand the energy in powers of  $1/\ell^2$ , and then determine the  $R$ -dependence by using Eqs. (3.9).

Let us first consider the supercurrent energy  $E_c$ , i.e., the second term in Eq. (2.16). It can be written

$$E_c/E_0 = \int_0^R dr r (\delta a(r))^2 = \frac{1}{\ell^6} \int_0^R dr r (\alpha(r/\ell))^2 + O(1/\ell^6). \quad (3.10)$$

Using Eqs. (3.5a) we find

$$E_c/E_0 = \frac{32}{5} \frac{1}{\ell^4} + O(1/\ell^6). \quad (3.11)$$

Now consider the magnetic energy  $E_m$ , which is the third term in Eq. (2.16). It can be written

$$E_m/E_0 = \int_0^R dr r b^2(r), \quad (3.12)$$

with

$$b(r) = \frac{1}{r} a_\infty(r) + a'_\infty(r) + \frac{1}{r} \delta a(r) + \delta a'(r), \quad (3.13a)$$

the magnetic induction in our reduced units. Notice that in calculating  $a_\infty(r)$ ,  $\theta(r)$  in Eq. (3.1) needs to be expanded to first order in  $\delta\theta$ , as noted earlier. The two leading contributions to  $b^2$  are then

$$b^2(r) = \frac{16}{\ell^4} \frac{1}{(1+x^2)^4} - \frac{8}{\ell^6} \frac{1}{(1+x^2)^2} \left[ 2 \frac{1-x^2}{x(1+x^2)^2} g(x) + \frac{2g'(x)}{1+x^2} + \frac{1}{x} \alpha(x) + \alpha'(x) \right] + O(1/\ell^8), \quad (3.13b)$$

where  $x = r/\ell$ . Performing the integral yields

$$E_m/E_0 = \frac{8}{3} \frac{1}{\ell^2} - \frac{112}{135} \frac{1}{\ell^4} + O(1/\ell^6). \quad (3.14)$$

Finally, we need to calculate the energy  $E_s$  coming from the gradient terms in the first term in Eq. (2.16). The expansion of the two terms in the integrand yields seven integrals that contribute to the desired order, they are listed in Appendix C. The result is

$$E_s/E_0 = 2 + \frac{8}{3} \frac{1}{\ell^2} + \frac{64}{9} \frac{\ln \ell}{\ell^4} + \left( -\frac{1,832}{135} - 2c\sqrt{2c}\delta + 4c^2 \ln(2/c) \right) \frac{1}{\ell^4} + O(1/\ell^6). \quad (3.15)$$

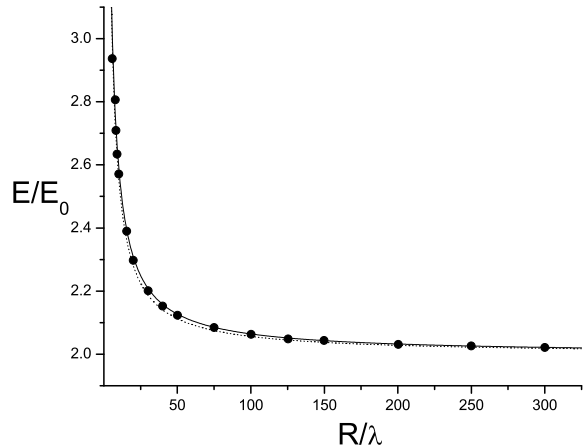


FIG. 6: Numerical data for the energy per skyrmion per unit length (circles) together with the best fit to a pure  $1/R$  behavior (dashed line) from Ref.<sup>16</sup>, and the perturbative analytic solution given by Eq. (3.16) (solid line). A numerical solution using spectral methods is indistinguishable from the perturbative one.

Adding the three contributions, and using Eqs. (3.9), we find our final result for the energy of a skyrmion of radius  $R \gg 1$ ,

$$E/E_0 = 2 + \frac{8\sqrt{6}}{3} \frac{1}{R} - \frac{16}{3} \frac{\ln R}{R^2} - \frac{4}{45} [7 + 30 \ln(3/2)] \frac{1}{R^2} + O(\ln^2 R/R^3). \quad (3.16)$$

Knigavko et al.<sup>16</sup> solved the Eqs. (2.17) numerically, and thereby numerically determined the energy, which they fit to a  $1/R$ -dependence. Their results are shown in Fig. 6 together with the analytical result given in Eq. (3.16). The perturbative solution up to  $O(\ln R/R^2)$  was first given in Ref. 21. We have also solved the equations numerically, using spectral methods to convert the boundary value problem to a set of algebraic equations for the unknown coefficients in an expansion in Chebyshev polynomials<sup>30</sup>. For the  $R$ -range shown, and on the scale of the figure, the result is indistinguishable from the perturbative one.

## IV. OBSERVABLE CONSEQUENCES OF THE SKYRMION ENERGY

Our calculation of the skyrmion energy in Sec. III has been for a cylindrically symmetric skyrmion. The result shows that each skyrmion will try to maximize its radius in order to minimize the energy, which leads to a repulsive interaction between skyrmions whose potential is proportional to  $1/R$ . Skyrmions are thus expected to

form a lattice structure, as do vortices, and they will thus *not* be cylindrically symmetric, since the lattice is not. One expects a hexagonal lattice, as in the case of the vortex lattice, and our treatment involves the same approximation as in the numerical work of Ref. 16; namely, approximating the hexagonal unit cell by a circle of the same area. We expect this approximation to recover the correct scaling of the energy, and to reproduce the coefficients of that scaling to the same accuracy as radius of the circle of the same area reproduces the distance from the center of a hexagon to the nearest point on its edge; i.e.,  $\sqrt{2\sqrt{3}/\pi} - 1 \approx 0.05$ . We will now proceed to calculate observable consequences of the dependence of the energy on the radius of the unit cell. These include the relation  $B(H)$  between the magnetic induction  $B$  and the external magnetic field  $H$ , the elastic properties of the skyrmion lattice and the resulting phase diagram in the  $H$ - $T$ -plane, and the  $\mu$ SR signature of the skyrmion lattice.

### A. $B(H)$ for a skyrmion lattice

We start by calculating the dependence of the equilibrium lattice constant  $R$  on an external magnetic field  $H$ . This is done by minimizing the energy per unit volume, which is the energy per unit length per skyrmion, Eq. (3.16), divided by the area per skyrmion,  $\pi R^2$ , plus a reduction in the energy of  $-2\Phi_0 H/4\pi$  due to the external field. The latter is obtained from the last term in Eq. (2.8) by noting that the magnetic flux  $\int dx dy (\hat{z} \cdot \mathbf{b}) = 2\Phi_0$  for each skyrmion in the lattice. This negative external field contribution must also be divided by  $\pi R^2$  to give the energy per unit volume. Returning to ordinary units, we thus find a Gibbs free energy per unit volume

$$g(R) = \frac{K}{4\pi^2} \left[ -\frac{\Delta}{R^2} + \frac{4\sqrt{6}\lambda}{3R^3} + O\left(\frac{\lambda^2 \ln(R/\lambda)}{R^4}\right) \right], \quad (4.1)$$

where  $K = \Phi_0^2/2\pi\lambda^2$ , and

$$\Delta \equiv 1 - H/H_{c1}, \quad (4.2)$$

with  $H_{c1} \equiv K/2\Phi_0$ . For  $H < H_{c1}$ , we have  $\Delta > 0$ , and the free energy is minimized by  $R = \infty$ ; i.e., the skyrmion density is zero. This is the Meissner phase. For  $H > H_{c1}$  the free energy is minimized by

$$R = R_0 = 2\sqrt{6}\lambda/\Delta, \quad (4.3)$$

and there is a nonzero skyrmion density. We see that  $H_{c1}$  is indeed the lower critical field. Note that the equilibrium flux lattice constant  $R_0$  diverges as  $1/\Delta$ , whereas in the case of a vortex lattice it diverges only logarithmically as  $\ln(1/\Delta)$ .<sup>1</sup> For the averaged magnetic induction  $B = 2\Phi_0/\pi R_0^2$  this implies

$$B(H) = \frac{1}{3} H_{c1} \Delta^2. \quad (4.4)$$

For  $H \rightarrow H_{c1}$  from above,  $B(H)$  in the case of a skyrmion lattice thus vanishes with zero slope, whereas in the case of a vortex lattice it vanishes with an infinite slope.<sup>1</sup> This result, with a slightly different prefactor, was first obtained from the aforementioned numerical determination of  $E(R)$  in Ref. 16. Note that the only material parameter that appears in this expression for  $B$  is  $H_{c1}$ .

### B. Elastic properties of the skyrmion lattice

Now we turn to the elastic properties of skyrmion lattice. Let the equilibrium position of the  $i^{\text{th}}$  skyrmion line be described by a two-dimensional lattice vector  $\mathbf{R}_i = (X_i, Y_i)$ , and the actual position by

$$\mathbf{r}_i(z) = (X_i + u_x(\mathbf{R}_i, z), Y_i + u_y(\mathbf{R}_i, z), z), \quad (4.5)$$

where  $\mathbf{u} = (u_x, u_y)$  is the two-dimensional displacement vector, and we use  $z$  as the parameter of the skyrmion line. The strain tensor  $u_{\alpha\beta}$  is defined as

$$u_{\alpha\beta}(\mathbf{x}) = \frac{1}{2} \left( \frac{\partial u_\alpha}{\partial x_\beta} + \frac{\partial u_\beta}{\partial x_\alpha} \right). \quad (4.6)$$

For a hexagonal lattice of lines parallel to the  $z$ -axis, the elastic Hamiltonian is<sup>31</sup>

$$H_{\text{el}} = \frac{1}{2} \int d\mathbf{x} \left[ 2\mu (u_{\alpha\beta}(\mathbf{x})u_{\alpha\beta}(\mathbf{x})) + \lambda_L (u_{\alpha\alpha}(\mathbf{x}))^2 + K_{\text{tilt}} |\partial_z \mathbf{u}(\mathbf{x})|^2 \right]. \quad (4.7)$$

Here summation over repeated indices is implied.  $\mu$ ,  $\lambda_L$ , and  $K_{\text{tilt}}$  are the shear, bulk, and tilt moduli, respectively, of the lattice, and we now need to determine these elastic constants.

The combination  $\mu + \lambda_L$  can be obtained by considering the energy change of the system upon a dilation of the lattice. Let  $R$  change from  $R_0$  to  $R_0(1 + \epsilon)$ , with a dilation factor  $\epsilon \ll 1$ . Such a dilation corresponds to a displacement field  $\mathbf{u}(\mathbf{x}) = \epsilon \mathbf{x}_\perp$ , where  $\mathbf{x}_\perp$  is the projection of  $\mathbf{x}$  perpendicular to the  $z$ -axis.<sup>31</sup> The strain tensor is thus  $u_{\alpha\beta} = \epsilon \delta_{\alpha\beta}$ . Inserting this in the elastic Hamiltonian, Eq. (4.7), yields the energy per unit volume for the dilation,

$$E_{\text{dil}}/V = 2(\mu + \lambda_L) \epsilon^2. \quad (4.8a)$$

This should be compared with the energy as given by Eq. (4.1),

$$\begin{aligned} E_{\text{dil}}/V &= g(R_0(1 + \epsilon)) - g(R_0) = \frac{1}{2} \left( \frac{\partial^2 g}{\partial R^2} \right)_{R_0} (\epsilon R_0)^2 \\ &= \frac{K \Delta^3}{96\pi^2 \lambda^2} \epsilon^2. \end{aligned} \quad (4.8b)$$

Comparing Eqs. (4.8a) and (4.8b) yields

$$\mu + \lambda_L = K \Delta^3 / 192\pi^2 \lambda^2. \quad (4.9)$$



To obtain  $\mu$  (or  $\lambda_L$ ) separately, we should consider shear deformations, which change the shape, but not the area, of the unit cell. Since we have already approximated the hexagonal unit cell by a circle, this is difficult to do, and we resort to the following heuristic method, which will give the correct scaling of  $\mu$  with  $\Delta$  (but not the correct prefactors). To this end we observe that our result for the Gibbs free energy, Eq. (4.1), is of the same form we would have obtained if the skyrmions interacted via a pair potential  $U(r)$  that for distances  $r \lesssim R_0$  is of order  $K\lambda/r$ , and for larger distances falls off sufficiently rapidly that only nearest-neighbor interactions need to be considered. Treating the skyrmion lattice as if such an “equivalent potential” were the origin of the skyrmion energy allows us to calculate the shear modulus as follows:

If the lattice is subjected to a uniform  $x-y$  shear - i.e., a displacement field  $\mathbf{u}(\mathbf{x}) = 2\epsilon y \hat{\mathbf{x}}$  - for which  $u_{xy} = u_{yx} = \epsilon$ , and all other components of  $u_{\alpha\beta} = 0$ , the elastic energy, Eq. (4.7) predicts an elastic energy per unit volume of

$$E/V = 2\mu\epsilon^2. \quad (4.10)$$

Such a shear skews each fundamental triangle of the skyrmion lattice by displacing the top (or bottom, for the downward-pointing triangles) to the right (or the left, for downward-pointing triangles) by an amount of order  $\epsilon R_0$ , where  $R_0$  is the skyrmion lattice spacing found earlier, Eq. (4.3) (see Fig. 7). This shortens the length of

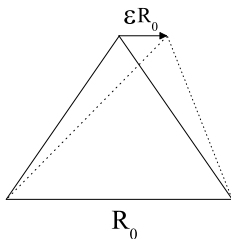


FIG. 7: Shearing of the skyrmion lattice results in a change in the distance between skyrmion centers, and hence in their effective interaction. See the text for additional information.

one bond of the triangle by an amount of order  $\epsilon R_0$ , and increases the opposite bond’s length by the same amount. Hence, the linear in  $\epsilon$  change in the “equivalent potentials” of these two bonds cancels, and the total change ( $\Delta E/\text{triangle}$ ) in the energy per unit length of fundamental triangle, per triangle, is given by:

$$\frac{\Delta E}{\text{triangle}} = U''(R_0)(\epsilon R_0)^2 \times O(1) \quad (4.11)$$

where the  $O(1)$  factor includes both geometrical factors (e.g., sines and cosines), and counting factors (e.g., to avoid multiple counting of each triangle). If we take

$U(r) = K\lambda/r$  as suggested above, we have

$$U''(R_0) = \frac{K\lambda}{R_0^3} \times O(1). \quad (4.12)$$

Inserting this into Eq. (4.11) gives

$$\frac{\Delta E}{\text{triangle}} = \frac{K\lambda}{R_0} \epsilon^2 \times O(1). \quad (4.13)$$

This is the change in energy per unit cell. To get the energy per unit volume, we must divide by the unit cell area, which is  $\pi R_0^2$ . Doing so gives

$$\frac{\Delta E}{V} = \frac{K\lambda}{R_0^3} \epsilon^2 \times O(1). \quad (4.14)$$

Comparing this with Eq. (4.10) then determines  $\mu$ :

$$\mu = \frac{K\lambda}{R_0^3} \times O(1). \quad (4.15)$$

Using Eq. (4.3) for  $R_0$  then leads to our final result for  $\mu$ :

$$\mu = \frac{K\Delta^3}{\lambda^2} \times O(1). \quad (4.16a)$$

From Eq. (4.9) we see that the bulk modulus or Lamé coefficient is given given by the same expression,

$$\lambda_L = \frac{K\Delta^3}{\lambda^2} \times O(1). \quad (4.16b)$$

We now turn to the tilt modulus  $K_{\text{tilt}}$ . This can be obtained by considering a uniform tilt of the axes of the skyrmions away from the  $z$ -axis, i.e., away from the direction of the external magnetic field  $H$ , by an angle  $\vartheta \ll 1$ . For small  $\vartheta$ ,  $\vartheta = |\partial\mathbf{u}/\partial z|$ . Therefore, the tilt energy in Eq. (4.7) is identical with the change of the  $\mathbf{B} \cdot \mathbf{H}$  term in Eq. (2.8). This contribution to the energy is, per unit length and in ordinary units, given by  $-\Phi_0 H \cos\theta/2\pi$ , and its change due to tilting is  $\Phi_0 H(1 - \cos\vartheta)/2\pi \approx \Phi_0 H \vartheta^2/4\pi = \Phi_0 H |\partial_z \mathbf{u}|^2/4\pi$ . Dividing this result by the unit cell area  $\pi R_0^2$ , using Eq. (4.3) for  $R_0$ , and identifying the result with the tilt term in the elastic Hamiltonian, Eq. (4.7), yields  $K_{\text{tilt}}$  in the vicinity of  $H_{c1}$ ,

$$K_{\text{tilt}} = \frac{1}{12\pi} H_{c1}^2 \Delta^2. \quad (4.17)$$

We now are in a position to calculate the mean-square positional fluctuations  $\langle |\mathbf{u}(\mathbf{x})|^2 \rangle$ . Taking the Fourier transform of Eq. (4.7), and using the equipartition theorem, yields

$$\langle |\mathbf{u}(\mathbf{x})|^2 \rangle_T = \frac{k_B T}{V} \sum_{\mathbf{q} \in \text{BZ}} \frac{1}{\mu q_1^2 + K_{\text{tilt}} q_z^2} \quad (4.18a)$$

for the transverse fluctuations, and

$$\langle |\mathbf{u}(\mathbf{x})|^2 \rangle_L = \frac{k_B T}{V} \sum_{\mathbf{q} \in \text{BZ}} \frac{1}{(2\mu + \lambda_L) q_1^2 + K_{\text{tilt}} q_z^2} \quad (4.18b)$$

for the longitudinal ones. Here  $q_{\perp}$  and  $q_z$  are the projections of the wave vector  $\mathbf{q}$  orthogonal to and along the  $z$ -direction, respectively. The Brillouin zone BZ of the skyrmion lattice is a hexagon (which we have approximated by a circle) of edge length  $O(1)/R_0$  in the plane perpendicular to the  $z$ -axis, and extends infinitely in the  $z$ -direction.

Since  $\mu$  and  $\lambda_L$  are the same apart from a prefactor of  $O(1)$  which we have not determined, see Eqs. (4.16), the same is true for the transverse and longitudinal contributions to the fluctuations, and it suffices to consider the former. Performing the integral over  $q_z$  yields

$$\begin{aligned} \langle |\mathbf{u}(\mathbf{x})|^2 \rangle &= \langle |\mathbf{u}(\mathbf{x})|^2 \rangle_L + \langle |\mathbf{u}(\mathbf{x})|^2 \rangle_T \\ &\propto \langle |\mathbf{u}(\mathbf{x})|^2 \rangle_T = \frac{k_B T}{\sqrt{\mu} K_{\text{tilt}}} \int_{\text{BZ}} \frac{d^2 q_{\perp}}{8\pi^2} \frac{1}{q_{\perp}}. \end{aligned} \quad (4.19)$$

The remaining integral over the perpendicular part of the Brillouin zone is proportional to  $1/R_0$ , and using Eqs. (4.16) and (4.3) we obtain

$$\langle |\mathbf{u}(\mathbf{x})|^2 \rangle = \frac{k_B T}{\lambda H_{c1}^2} \frac{1}{\Delta^{3/2}} \times O(1). \quad (4.20)$$

Using Eq. (4.3) again we see that, near  $H_{c1}$ ,  $\langle |\mathbf{u}(\mathbf{x})|^2 \rangle \propto R_0^{3/2} \ll R_0^2$ . That is, in this regime the positional fluctuations are small compared to the lattice constant, which tells us that the lattice will be stable against melting. To elaborate on this, let us consider the Lindemann criterion for melting, which states that the lattice will melt when the ratio  $\Gamma_L = \langle |\mathbf{u}(\mathbf{x})|^2 \rangle / R_0^2$  exceeds a critical value  $\Gamma_c = O(1)$ . In our case,

$$\Gamma_L = \frac{k_B T}{H_{c1}^2 \lambda^{5/2}} \Delta^{1/2} \times O(1). \quad (4.21)$$

As  $H \rightarrow H_{c1}$ ,  $\Delta \rightarrow 0$ , and the Lindemann ratio vanishes. Hence, the skyrmion lattice does not melt at any temperature for  $H$  close to  $H_{c1}$ .

We finally determine the shape of the melting curve  $H_m(T)$  near the superconducting transition temperature  $T_c$ . Since, in mean field theory,  $H_{c1} \propto (T_c - T)$ , and  $\lambda \propto 1/\sqrt{T_c - T}$ ,<sup>1</sup> we find from Eq. (4.21) by putting  $\Gamma_L = \text{const.} = O(1)$ ,

$$H_m - H_{c1} \propto (T_c - T)^{5/2}. \quad (4.22)$$

The resulting phase diagram is shown schematically in Fig. 8. Comparing with Fig. 1 we see the qualitative difference between the vortex and skyrmion flux lattices: whereas the vortex lattice always melts near  $H_{c1}$ , the skyrmion lattice melts nowhere near  $H_{c1}$ . This is a direct consequence of the long-ranged interaction between skyrmions, as opposed to the screened Coulomb interaction between vortices.

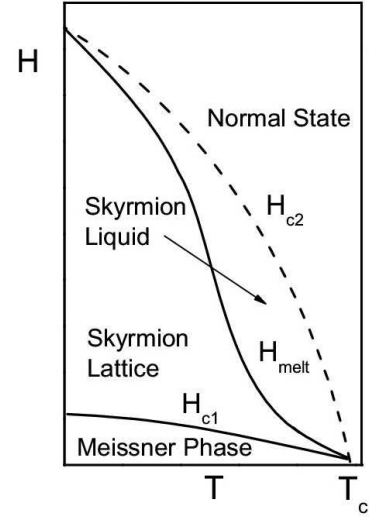


FIG. 8: External field ( $H$ ) vs. temperature ( $T$ ) phase diagram for skyrmion flux lattices. In contrast to the vortex case, see Fig. 1, there is a direct transition from the skyrmion lattice to the Meissner phase. The theory predicts the shape of the melting curve only close to  $T_c$ , see Eq. (4.22); the rest of the curve is an educated guess.

### C. $\mu$ SR signature of a skyrmion flux lattice

Muon spin rotation ( $\mu$ SR) is a powerful tool which has been extensively applied to study the vortex state in type-II superconductors.<sup>32,33</sup> A crucial quantity in this type of experiment is the  $\mu$ SR line shape  $n(B)$ , which is the probability density that a muon experiences a local magnetic induction  $B$  and precesses at the Larmor frequency that corresponds to  $B$ . It is defined as

$$n(B) \equiv \langle \delta(B(\mathbf{x}) - B) \rangle, \quad (4.23)$$

where  $B(\mathbf{x})$  is the magnitude of the local magnetic induction, and  $\langle \dots \rangle$  denotes the spatial average over a flux lattice unit cell.

To predict the  $\mu$ SR line shape for a skyrmion flux lattice near  $H_{c1}$  it is sufficient, for large  $R_0$ , to use only the lowest solution for the magnetic induction obtained in Sec. III A. Inserting Eqs. (3.3) into Eq. (3.1), we find for the magnetic induction in reduced units

$$b(r) = -\frac{4\ell^2}{(r^2 + \ell^2)^2}. \quad (4.24)$$

Restoring physical units then gives

$$B(r) = \frac{H_{c1}\lambda^2}{2} \frac{\ell^2}{(r^2 + \ell^2)^2}, \quad (4.25)$$

where we've dropped the minus sign since only the magnitude of  $B$  can be detected in  $\mu$ SR measurements.

From Eq. (4.23) we then find, for  $H$  near  $H_{c1}$ , where our theory is valid,

$$n(B) = \frac{1}{24\sqrt{2}} \left( \frac{H_{c1}\Delta}{B} \right)^{\frac{3}{2}} \frac{1}{H_{c1}} \quad (\text{skyrmions}). \quad (4.26)$$

Of course,  $n(B)$  is only non-zero for those values of  $B$  that actually occur inside the unit cell of the skyrmion lattice. From Eq. (4.25), we see that the maximum value of  $B$  will occur at the center of the unit cell ( $r = 0$ ), which gives

$$|B|_{\max} = |B(r = 0)| = \frac{H_{c1}\lambda^2}{2\ell^2} = \frac{H_{c1}\Delta}{8}, \quad (4.27a)$$

The minimum value of  $B$  occurs at the edge of the unit cell (i.e.,  $r = R$ ), where Eq. (4.25) gives

$$|B|_{\min} = |B(r = R)| = \frac{H_{c1}\lambda^2\ell^2}{2R^4} = \frac{H_{c1}\Delta^3}{288}. \quad (4.27b)$$

In the second equalities in Eqs. (4.27) we have used Eqs. (3.9) and (4.3) to express  $\ell$  in terms of  $R$  and  $R$  in terms of  $\Delta$ , respectively.

To summarize: the prediction of our cylindrical approximation for  $n(B)$  is that the simple power law Eq. (4.26) holds for  $B_{\min} < B < B_{\max}$ . For  $B < B_{\min}$  or  $B > B_{\max}$ ,  $n(B) = 0$ .

Since the above results were derived in the cylindrical approximation, we expect the numerical coefficients in Eqs. (4.27) to be off by the approximately 5% mentioned in the opening paragraph of Sec. IV throughout most of the range  $B_{\min} < B < B_{\max}$ . When  $B$  gets close to  $B_{\min}$ , however, we expect more radical departures from the cylindrical approximation. This is because contours of constant  $B$  near the edge of the hexagonal unit cell will, for  $B$  within 5% or so of  $B_{\min}$  or so, start intersecting the unit cell boundary, leading to van Hove-like singularities in  $n(B)$ . Such subtleties cannot be captured within the cylindrical approximation. Note, however, that they only occur over a very small range of  $B$ ; for the remainder of the large window  $B_{\min} < B < B_{\max}$  (which spans three decades even for  $\Delta$  as big as 0.2), Eq. (4.26) holds, up to the aforementioned 5% numerical error in its overall coefficient.

To compare this result with the corresponding one for a vortex flux lattice, we recall that in that case  $B(r)$  is given by a modified Bessel function which for distances  $r \gg \lambda$  takes the form

$$B(r) \propto \frac{1}{\sqrt{r/\lambda}} e^{-r/\lambda}. \quad (4.28)$$

For small  $B$ , we then find from Eq. (4.23)

$$n(B) \propto \frac{\ln(1/B)}{B} \quad (\text{vortices}). \quad (4.29)$$

We see that the  $\mu$ SR line shape is qualitatively different in the two cases, due to the long-range nature of  $B(r)$  in the skyrmion case versus the exponential decay in the vortex case.

## V. CONCLUSION

In summary, we have considered properties of a flux lattice formed by the topological excitations commonly

referred to as skyrmions, rather than by ordinary vortices. For strongly type-II materials in the  $\beta$ -phase, skyrmions are more stable than vortices.<sup>16</sup> We have presented an analytical calculation of the energy of a cylindrically symmetric skyrmion of radius  $R$  up to  $O(1/R^2)$  in an expansion in powers of  $1/R$ . This provides excellent agreement with numerical solutions of the skyrmion equations. The interaction between skyrmions is long-ranged, falling off only as the inverse distance, in contrast to the exponentially decaying interaction between vortices. As a result, the elastic properties of a skyrmion flux lattice are very different from those of a vortex flux lattice, which leads to qualitatively different melting curves for the two systems. The phase diagram thus provides a smoking gun for the presence of skyrmions. In addition, the  $\mu$ SR line width for skyrmions is qualitatively different from the vortex case.

We finally mention two limitations of our discussion. First, we have restricted ourselves to a discussion of a particular  $p$ -wave ground state, namely, the non-unitary state sometimes referred to as the  $\beta$ -phase. This state breaks time-reversal symmetry and the recently reported absence of experimental evidence for the latter in  $\text{Sr}_2\text{RuO}_4$ <sup>34</sup> suggests to also consider other possible  $p$ -wave states and their topological excitations, in analogy to the rich phenomenology in Helium 3.<sup>11</sup> Second, in a real crystalline material, crystal-field effects will invalidate our isotropic model at very long distances, and cause the skyrmion interaction to fall off exponentially. This is the same effect that makes, for instance, the isotropic Heisenberg model of ferromagnetism inapplicable at very long distances and gives the ferromagnetic magnons a small mass. It should be emphasized that this is usually an extremely weak effect that is also material dependent. Once  $p$ -wave superconductivity has been firmly established in a particular material, this point needs to be revisited in order to determine the energy scales on which the above analysis is valid.

## Acknowledgments

We thank Tom Devereaux for suggesting the discussion of  $\mu$ SR as a possible probe for skyrmion lattices, and Hartmut Monien for a discussion on defects in Helium 3. Part of the work was performed at the Aspen Center for Physics. This work was supported by the NSF under grant No. DMR-05-29966.

## APPENDIX A: PROPERTIES OF ORTHOGONAL UNIT VECTORS

Let  $\hat{n}$  and  $\hat{m}$  be orthogonal real unit vectors, and  $\hat{l} = \hat{n} \times \hat{m}$ . Then the normalization condition  $\hat{n}_i \hat{n}_i = \hat{m}_i \hat{m}_i =$

1 and the orthogonality condition  $\hat{n}_i \hat{m}_i = 0$  imply

$$\hat{n}_j \partial_i \hat{n}_j = \hat{m}_j \partial_i \hat{m}_j = 0, \quad (\text{A1a})$$

$$\hat{n}_j \partial_i \hat{m}_j = -\hat{m}_j \partial_i \hat{n}_j. \quad (\text{A1b})$$

With these relations it is straightforward to show that

$$\partial_i \hat{n}_j \partial_i \hat{n}_j + \partial_i \hat{m}_j \partial_i \hat{m}_j = 2(\hat{n}_j \partial_i \hat{m}_j)(\hat{n}_k \partial_i \hat{m}_k) + \partial_i \hat{l}_j \partial_i \hat{l}_j. \quad (\text{A2})$$

Finally, in regions where  $\hat{l}(\mathbf{x})$  is differentiable the Mermin-Ho relation<sup>35</sup> holds,

$$\hat{l} \cdot (\partial_i \hat{l} \times \partial_j \hat{l}) = \partial_i \hat{n} \cdot \partial_j \hat{m} - \partial_i \hat{m} \cdot \partial_j \hat{n}. \quad (\text{A3})$$

## APPENDIX B: SOLUTIONS OF THE ODEs FOR $g$ AND $h$

The functions  $g$  and  $h$  in Sec. IIIB both satisfy an ODE of the form (see Eqs. (3.6))

$$F''(x) + \frac{1}{x} F'(x) - \frac{(x^4 - 6x^2 + 1)}{x^2(1+x^2)^2} F(x) = q(x), \quad (\text{B1})$$

with an inhomogeneity  $q$  given by the right-hand side of Eq. (3.6a) or (3.6b), respectively. It is easy to check that the corresponding homogeneous equation, obtained from Eq. (B1) by putting  $q(x) \equiv 0$ , is solved by

$$F_h(x) = x/(1+x^2). \quad (\text{B2})$$

(This is the solution that vanishes as  $x \rightarrow 0$ . The second solution diverges in this limit.) Now write  $F(x) = F_h(x)G(x)$ , and let  $y(x) = G'(x)$ . Then  $y$  is found to obey the elementary first-order ODE

$$y'(x) + p(x)y(x) = q(x)/F_h(x), \quad (\text{B3a})$$

with

$$p(x) = [2F_h'(x) + F_h(x)/x]/F_h(x). \quad (\text{B3b})$$

The solution is

$$y(x) = e^{-\int dx p} \left[ C_1 + \int dx q e^{\int dx p} \right], \quad (\text{B4})$$

with  $C_1$  an integration constant. A second integration yields  $G(x)$ , and hence  $F(x)$  in terms of two integration constants. The latter can be determined by requiring that for small  $x$  the solution coincides with the asymptotic solution that vanishes as  $x \rightarrow 0$ . By using a power-law ansatz for  $g$  and  $h$  in Eqs. (3.6) we find  $g(x \rightarrow 0) = -8x^3 + O(x^4)$ , and  $h(x \rightarrow 0) = 256x^3 + O(x^4)$ , which suffices to fix the integration constants. For  $g(x)$  we find the expression given in Eq. (3.7a). For  $h(x)$  we obtain

---


$$h(x) = \frac{1}{(270x(1+x^2)^4)} \left\{ 592 + 2x^2 [8(-1, 119 + 90x^2 + 286x^4 + 240x^6 + 30x^8) + 10, 320(1+x^2)^3] \right. \\ + 2, 296(-1+x^2)(1+x^2)^4 + 4x^2(1+x^2)^3 + 1, 704 \ln x \\ + 32 \ln(1+x^2) [-30 + 142x^2 + 276x^4 + 171x^6 + 52x^8 - 15x^{10} - 15(3+x^2)(x+x^3)^2 \ln(1+x^2)] \\ \left. - 1, 920x^2(1+x^2)^3 \text{Li}_2(-x^2) \right\}, \quad (\text{B5})$$


---

with  $\text{Li}$  the polylogarithm function. The asymptotic behavior for large  $x$  is given by Eq. (3.8).

## APPENDIX C: CONTRIBUTIONS TO $E_s$

By expanding the integrand of the first term in Eq. (2.16), we can express the energy  $E_s$  to  $O(1/R^2)$  in terms of seven integrals,

$$E_s/E_0 = \sum_{i=1}^7 I_i + O(1/\ell^6), \quad (\text{C1})$$

with

$$I_1 = 4 \int_0^{R/\ell} dx \frac{x}{(1+x^2)^2}, \quad (\text{C2a})$$

$$I_2 = \frac{2}{\ell^2} \int_0^{R/\ell} dx \frac{1}{1+x^2} \left( \frac{(x^2-1)}{x^2+1} g(x) - xg'(x) \right), \quad (\text{C2b})$$

$$I_3 = \frac{1}{2\ell^4} \int_0^{R/\ell} dx \left[ x(g'(x))^2 + \frac{(x^4-6x^2+1)}{x(1+x^2)^2} g^2(x) \right], \quad (\text{C2c})$$

$$I_4 = \frac{2}{\ell^4} \int_0^{R/\ell} dx \frac{1}{1+x^2} \left( \frac{(x^2-1)}{x^2+1} h(x) - xh'(x) \right), \quad (\text{C2d})$$

$$I_5 = \frac{1}{\ell^6} \int_0^{R/\ell} dx \left( xg'(x)h'(x) + \frac{(x^4-6x^2+1)}{x(1+x^2)^2} g(x)h(x) \right), \quad (\text{C2e})$$

$$I_6 = -\frac{4}{3\ell^6} \int_0^{R/\ell} dx \frac{(x^2-1)}{(1+x^2)^2} g^3(x), \quad (\text{C2f})$$

$$I_7 = -\frac{1}{6\ell^8} \int_0^{R/\ell} dx \frac{(x^2-1)^2}{x(1+x^2)^2} g^4(x). \quad (\text{C2g})$$

Evaluating the integrals to  $O(1/\ell^4)$  yields Eq. (3.15).

- 
- <sup>1</sup> M. Tinkham, *Introduction to Superconductivity* (McGraw-Hill, New York, 1975).
- <sup>2</sup> B. A. Huberman and S. Doniach, Phys. Rev. Lett. **43**, 950 (1979).
- <sup>3</sup> D. S. Fisher, Phys. Rev. B **22**, 1190 (1980).
- <sup>4</sup> D. R. Nelson and H. S. Seung, Phys. Rev. B **39**, 9153 (1989).
- <sup>5</sup> E. H. Brandt, Phys. Rev. Lett. **63**, 1106 (1989).
- <sup>6</sup> P. L. Gammel, L. F. Schneemeyer, J. V. Wasczak, and D. J. Bishop, Phys. Rev. Lett. **61**, 1666 (1988).
- <sup>7</sup> H. Safar, P. L. Gammel, D. H. Huse, D. J. Bishop, J. P. Rice, and D. M. Ginsberg, Phys. Rev. Lett. **69**, 824 (1992).
- <sup>8</sup> T. Skyrme, Proc. Roy. Soc. A **260**, 127 (1961).
- <sup>9</sup> Defects of this general type are known under various names in different contexts, and the action for the defects studied here differs from the one considered by Skyrme. We follow a recent trend to refer to all defects of this type as skyrmions.
- <sup>10</sup> P. W. Anderson and G. Toulouse, Phys. Rev. Lett. **38**, 508 (1977).
- <sup>11</sup> M. M. Salomaa and G. E. Volovik, Rev. Mod. Phys. **59**, 533 (1987).
- <sup>12</sup> D. C. Wright and N. D. Mermin, Rev. Mod. Phys. **61**, 385 (1989).
- <sup>13</sup> S. L. Sondhi, A. Karlhede, S. A. Kivelson, and E. H. Rezayi, Phys. Rev. B **47**, 16419 (1993).
- <sup>14</sup> C. Timm, S. M. Girvin, and H. A. Fertig, Phys. Rev. B **58**, 10634 (1998), and references therein.
- <sup>15</sup> U. Roessler, A. Bogdanov, and C. Pfleiderer, Nature **442**, 797 (2006).
- <sup>16</sup> A. Knigavko, B. Rosenstein, and Y. F. Chen, Phys. Rev. B **60**, 550 (1999).
- <sup>17</sup> K. D. Nelson, Z. Q. Mao, Y. M. Maeno, and Y. Liu, Science **306**, 1151 (2004).
- <sup>18</sup> M. Rice, Science **306**, 1142 (2004).
- <sup>19</sup> The precise nature of the order parameter in Sr<sub>2</sub>RuO<sub>4</sub> is still being debated, see Ref. 34.
- <sup>20</sup> Reference 16 focused on UPt<sub>3</sub>, which was the leading candidate for a *p*-wave superconductor at the time, but is now believed to have *f*-wave symmetry.
- <sup>21</sup> Q. Li, J. Toner, and D. Belitz, Phys. Rev. Lett. **98**, 187002 (2007).
- <sup>22</sup> The complete order parameter in a *p*-wave superconductor, or in <sup>3</sup>He, also contains an orbital sector, see Ref. 23. For our present purposes the orbital sector is of no importance, and we consider the spin sector only.
- <sup>23</sup> D. Vollhardt and P. Wölfle, *The Superfluid Phases of Helium 3* (Taylor & Francis, 1990).
- <sup>24</sup> See the discussion in Ref. 16, and references therein.
- <sup>25</sup> J. Zinn-Justin, *Quantum Field Theory and Critical Phenomena* (Oxford University Press, Oxford, 1996).
- <sup>26</sup> More generally,  $\phi$  is an element of the circle or one-sphere  $S_1$ , and hence  $\oint_C d\ell \cdot \nabla \phi(x) = 2\pi n$  with  $n$  an integer.  $n$  is a topological invariant that characterizes the singularity (known as a vortex), and the number of flux quanta that penetrate the vortex is  $N = |n|$ . The vortex with  $n = 1$  has the lowest energy within this family of solutions (apart from the trivial “non-vortex” with  $n = 0$ ).
- <sup>27</sup> R. Rajaraman, *Solitons and Instantons* (North-Holland, Amsterdam, 1982).
- <sup>28</sup> More generally,  $\int dx dy \epsilon_{ij} \hat{l} \cdot (\partial_i \hat{l} \times \partial_j \hat{l}) = 8\pi Q$ , with  $Q$  an integer.  $Q$  is a topological invariant that characterizes the defect (known as a skyrmion), and the number of flux quanta that penetrate the skyrmion is  $N = 2Q$ .<sup>16</sup> The skyrmion with  $Q = 1$  has the lowest energy within this family of solutions.
- <sup>29</sup> We emphasize that we do *not* require  $|\delta\theta(r)| \ll |\theta_\infty(r)|$ , as this requirement is neither necessary nor desirable. Rather, we expand, for instance,  $\sin(\theta_\infty + \delta\theta) = \sin\theta_\infty \cos\delta\theta + \cos\theta_\infty \sin\delta\theta = \cos\theta_\infty \delta\theta + O(\delta\theta^2)$ , which is valid for *all*  $\delta\theta \ll 1$ , *not* just for those that satisfy  $|\delta\theta(r)| \ll |\theta_\infty(r)|$ .
- <sup>30</sup> J. P. Boyd, *Chebyshev & Fourier Spectral Methods* (Springer, Berlin, 1989).
- <sup>31</sup> L. D. Landau and E. M. Lifshitz, *Theory of Elasticity* (Pergamon, Oxford, 1986).
- <sup>32</sup> J. E. Sonier, J. H. Brewer, and R. F. Kiefl, Rev. Mod. Phys. **72**, 769 (2000).
- <sup>33</sup> A. Schenck, *Muon Spin Rotation: Principles and Applications in Solid State Physics* (Adam Hilger, Bristol, 1986).
- <sup>34</sup> P. G. Björnsson, Y. Maeno, M. E. Huber, and K. A. Moler, Phys. Rev. B **72**, 012504 (2005).
- <sup>35</sup> N. D. Mermin and T.-L. Ho, Phys. Rev. Lett. **36**, 594 (1976).